

ABSOLUTE LUMINOSITY AND ENERGY DETERMINATION  
IN BUNCHED COLLIDING BEAM MACHINESRolland Johnson  
Fermilab, Batavia, IL. 60510

## 1 INTRODUCTION

The determination of the two basic machine parameters, energy and luminosity, which are needed for high energy physics analysis is the subject of this paper.

There is a basic difference between electron-positron machines and proton-antiproton colliders which should be made clear at the outset. First, because electrons and positrons are simple objects which interact via the electroweak force, their interaction cross sections into explicit final states can be calculated very precisely. Thus, for example, if elastic  $e^+e^-$  scattering (Bhabha) can be monitored at a physics detector, one has a measure of the machine luminosity. The energy of an  $e^+e^-$  machine does not come so easily and is of tremendous importance as it is a constraint on the final state detected in the experiment.

In a hadron-hadron collider, on the other hand, the absolute energy determination is relatively unimportant. This follows from the constituent nature of the proton and antiproton. Since these hadrons are made up of a collection of quarks and gluons (partons) which share the beam momentum, an interaction is really between one parton in each of the beams; the total energy in that interaction is only loosely related to the energy of the beams. Furthermore, since hadronic cross sections other than Coulomb scattering are not precisely calculable, reaction rates do not serve as absolute luminosity monitors.

In the following, only bunched beam operation is considered. This is a remarkable omission especially considering the tremendous success of the ISR, an unbunched proton-proton machine which used a novel luminosity measuring technique (the "van der Meer method").

Published in proceedings CERN-USA Accelerator School, Capri, Italy,  
Sept. 1988

## 2 LUMINOSITY

The number of events per second,  $R$ , which occur at an intersection region of a collider is simply related to the luminosity,  $L$ , and the production cross section,  $\sigma_{\text{tot}}$ . For a detector which is sensitive to scattered particles reasonably close to the circulating beams, the observed cross section is near 50 millibarns for collisions of 900 GeV protons on 900 GeV pbars. A luminosity of  $10^{30} \text{ cm}^{-2} \text{ s}^{-1}$  will yield 50,000 events per second into this detector. Thus, if one can measure the production cross section and the counting rate in a detector, one can determine the absolute luminosity of the machine.

$$R = L \sigma_{\text{tot}}$$

### 2.1 Luminosity from bunch and lattice parameters

A simple geometrical argument allows one to express  $L_{\text{cross}}$ , the luminosity per bunch-bunch crossing, as a function of the number of particles or antiparticles per bunch,  $N$  or  $\bar{N}$ , and the rms beam radius,  $a$ . The factor of 4 in the denominator comes from the assumption of beam distributions which are bi-Gaussian in the horizontal and vertical planes.

$$L_{\text{cross}} = \frac{N \bar{N}}{4 \pi a^2}$$

This is the luminosity per crossing of two bunches. To get the luminosity per revolution as seen at a particular interaction region (IR),  $L_{\text{cross}}$  for each pair of particle and antiparticle bunches which meet at the IR must be summed. The luminosity per second follows by multiplying the sum by the revolution frequency,  $f_{\text{rev}}$ .

There are corrections to this equation which are usually not discussed. The first is the observation that the intensities and profiles (both longitudinal and transverse) are usually different for each bunch of particles. To find the luminosity at a particular interaction region, one must use the parameters of the bunches which really collide there. The second correction involves the fact that the effective transverse beam size is a function of the strength of the focusing quadrupoles near the beam-beam crossing point. What this means is that a proper convolution of the longitudinal beam distributions must be made with the actual beta functions.

Only in exceptional cases can the beam size be determined at the interaction region where the experiment of interest is located. Usually the transverse rms invariant beam emittance  $\epsilon$  is measured at some other place in the lattice. The beam size in each plane is then given by:

$$a = \sqrt{\beta^* \epsilon} = \sqrt{\beta^* \epsilon_N m c / p}$$

where the relationship between the actual emittance and the normalized emittance is expressed in terms of the mass,  $m$ , and momentum,  $p$ , of the particle.

Since the interaction region occupies a drift space of the lattice, the focusing can be expressed by a quadratic in the longitudinal displacement from the center of the IR, where the (minimum)  $\beta^*$  occurs,  $\beta(s) = \beta^* + s^2/\beta^*$ .

#### BETA AND DISPERSION FUNCTION IN THE INTERACTION REGION

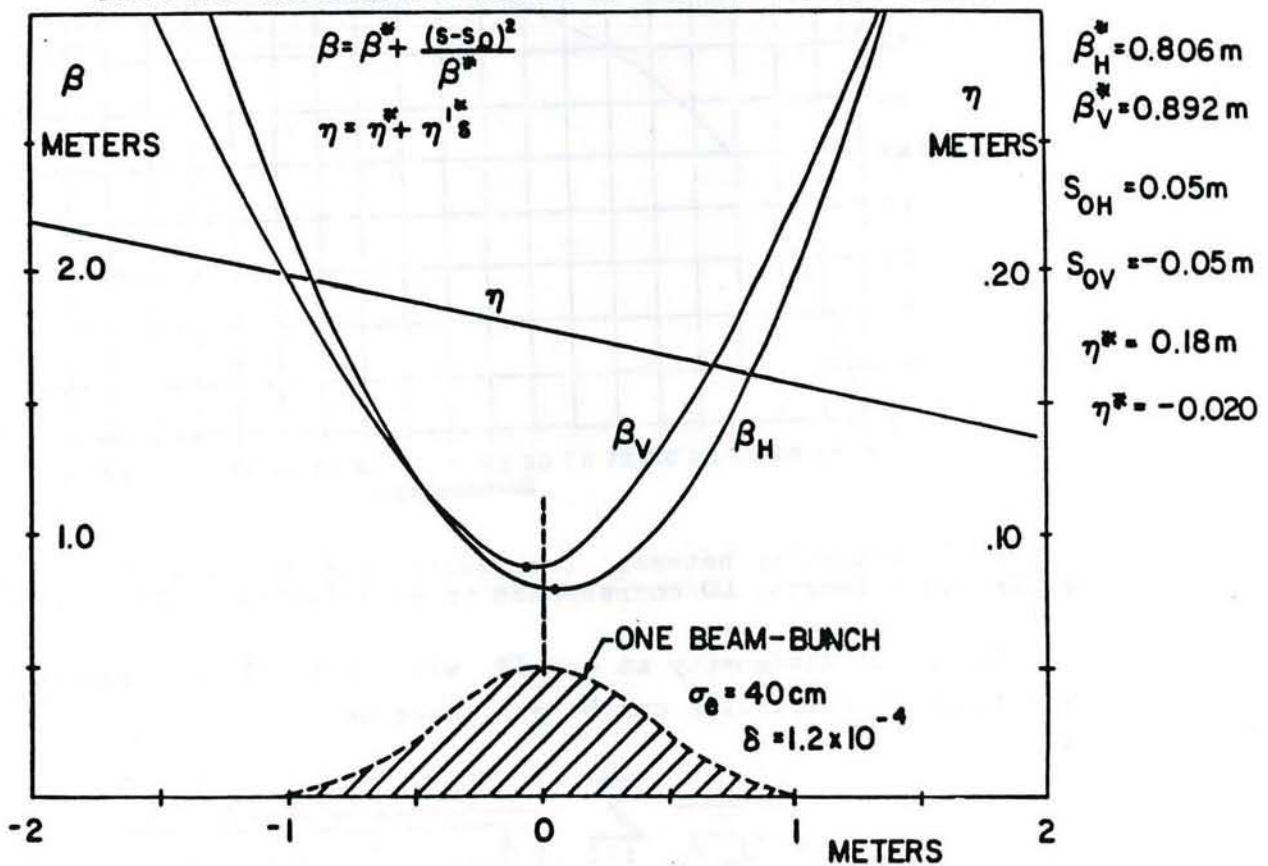


Fig. 1 Lattice parameters at the Tevatron BO interaction region. The length of the bunches is indicated.

Figure 1 shows the expected interaction distribution for the design parameters of the Tevatron Collider. The convolution integral over the longitudinal beam distribution can be done numerically, but tricks can be used to get an analytic expression which works well in all practical

cases. Assuming that the overlap region has a triangular rather than Gaussian longitudinal distribution yields the following expression for the luminosity degradation factor:

$$F = \frac{2 \tan^{-1} z}{z} - \frac{\log(1 + z^2)}{z^2}, \text{ where } z = \frac{2}{2 \beta_x^* \beta_y^*} \sqrt{\sigma_\lambda^2 + \sigma_\lambda^{-2}}$$

This bunch length degradation factor due to the fact that the bunch length is long relative to  $\beta^*$  is shown in figure 2. In this figure the horizontal and vertical beam sizes are assumed equal and the particle and antiparticle bunch lengths are also equal.

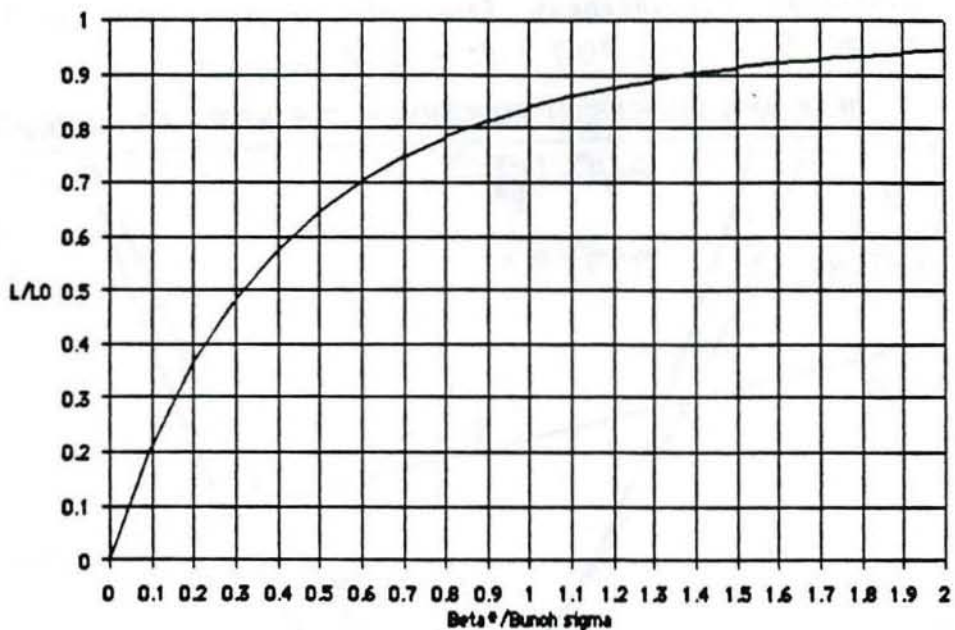


Fig. 2 Relationship between luminosity and  $\beta^*$ . Here  $\beta^*$  is normalized to the bunch length.  $L_0$  corresponds to an infinitesimally short bunch.

The total luminosity at one IR with  $n$  bunches of particles and  $n$  bunches of antiparticles can be expressed as:

$$L = \frac{f_{rev}}{4 \pi \sqrt{\beta_x \beta_y}} \sum_{i=1}^n \frac{N_i \bar{N}_j F(\sigma_{\lambda i}, \sigma_{\lambda j}, \beta_x^*, \beta_y^*)}{\sqrt{\frac{1}{4} (\epsilon_{xi} + \bar{\epsilon}_{xi})(\epsilon_{yi} + \bar{\epsilon}_{yi})}}$$

The subscript  $j = i + p$ , where  $p$  is a constant that depends on the bunch numbering scheme and the particular IR of interest. The  $\sigma_\lambda$  are bunch lengths of the  $i$ th and  $j$ th bunches of particles and antiparticles, respectively. The transverse emittances,  $\epsilon_x$  and  $\epsilon_y$ , are each averaged for particles and antiparticles. In this case the

emittances are not the normalized emittances, but those scaled for the energy of the collider. It is an easy exercise for the reader to show that if the normalized emittances and betas are equal, the luminosity will scale with the momentum of the beams, a fact of some significance when comparing the SppS with the Tevatron.

The expression above for the total luminosity was derived assuming that the dispersion at the crossing point is zero. Low  $\beta$  insertions are designed to keep the machine dispersion function and its derivative as close to zero as possible over the interaction region. This is approximately true for the B0 low  $\beta$  insertion at the Tevatron ( $\eta = 0.19$  m,  $\eta' = -0.143$ ), but even these small numbers affect the beam size at the crossing point. The modified expression is easy to derive. [11]

So now seeing all the components of a measurement of the luminosity based on intensities, emittances, and lattice functions, we can comment on how well you could do in the real world. At the Tevatron and the SPS the intensities and lengths of each bunch are measured with a resistive wall monitor, the transverse profiles are measured with a flying wire monitor, and the beta functions are inferred from SYNCH calculations and checked by measurements of betatron tunes as a function of single quadrupole strengths. Perhaps the biggest uncertainty at the Tevatron is the knowledge of the transverse beam sizes at the IR.

The transverse emittance of the bunches is determined using flying wire measurements at some convenient locations in the lattice. In the Tevatron, where much of the beam pipe is surrounded by cryogenic components of one sort or another, there are relatively few locations where the environment is suitable for a wire scanner. For the best measurements, one would prefer a location where the  $\beta$  function is large in the plane of interest to minimize effects from the finite resolution of position encoders. One also prefers to have separate wire scanners which are as independently sensitive to transverse emittance and dispersion as possible. These requirements are rarely satisfied simultaneously, especially considering that the scanners must work for different lattice configurations (e.g. with the low  $\beta$  on or off).

What is usually done in the horizontal plane is to use two wire scanners at different locations which have different beta functions and different dispersion functions. The horizontal beam size as measured at positions 1 and 2 is due to the combination of the transverse emittance

and the momentum spread of the beam:

$$a_{1,2}^2 = \beta_{1,2} \epsilon_x + \left[ \eta_{1,2} \frac{\Delta p}{p} \right]^2$$

The two equations can be solved to yield the horizontal emittance and the momentum spread. This method works well if the profiles as seen by the wire scanners are simple enough to be characterized by a single number,  $a$ . What can be done to gain some confidence that the measurement is valid is to compare the momentum spread measured by this technique to the momentum spread determined by the bunch length measured from the sampling scope monitor of the resistive wall pick up and the rf voltage.

The bucket area in eV-s is

$$A = \alpha(\Gamma) \frac{16 R}{c} \sqrt{\frac{e V E}{2 \pi h^3 \eta}},$$

where  $\alpha(\Gamma = \sin \phi_s) = 1$  for a stationary bucket,  $eV$  is the rf voltage,  $h$  is the harmonic number of the Tevatron rf (1113), and

$$\eta = \frac{1}{\gamma_t^2} - \frac{1}{\gamma^2} \approx \frac{1}{18.8^2}, \text{ for the Tevatron.}$$

TEVATRON LUMINOSITY CALCULATION						♦FTP♦COPIES♦		
STORE 1635	CMA100% mini lattice				10/03/88 12:23:37			
*READ DataBase	*CALC EMITS	*CALC LUMS			*STORE IN DB	LAST FLY		
SBD Data and Flying Wire Sigmas						95% trans emittance and rms DP/P		
SBint	SBsig	HA17	HC48	VC48	vert	horiz	DP/P	
p1	53.2	51	1.148	.6707	.4611	17.65	.144	.141
p2	53.8	51	1.142	.6321	.4414	16.17	.146	.141
p3	56.2	52	1.106	.6296	.4374	15.88	.140	.143
p4	53.1	48	1.08	.6432	.4467	16.56	.135	.133
p5	51.3	48	1.097	.6467	.4406	16.12	.137	.133
p6	64.1	50	1.082	.6255	.44	16.07	.136	.138
	(E9)	(cm)	(mm)	(mm)	( $\pi$ mmmr)	( $\pi$ mmmr)	(E-3)	(E-3)
a1	25.1	42	1.009	.6447	.4598	17.55	.122	.116
a2	25	43	1.026	.627	.451	16.88	.127	.119
a3	27	44	1.025	.6373	.4536	17.08	.126	.122
a4	26	44	1.001	.6396	.4647	17.93	.121	.122
a5	25.3	43	1.043	.6493	.469	18.26	.128	.119
a6	22.8	44	1.051	.6566	.4746	18.70	.129	.122
ENERGY=	900	Q1=	4283	p avg	16.41	11.37	.140	.138
RFSUM =	1.132	RA=	1.128	pbar "	17.73	11.41	.125	.120
				Ltot	B0	C0	E0	
.806	.804	.805	.815	.812	.80	1.806E+30	9.581E+27	2.419E+28
B0 Bunch Length Corrections						BOLUMP= 1.46 E+30		
LUMINOSITY AT STRAIGHT SECTIONS								
p1	p2	p3	p4	p5	p6	a		
B0	2.746E+29	2.593E+29	3.088E+29	2.947E+29	3.044E+29	3.648E+29	561234	
C0	1.473E+27	1.600E+27	1.796E+27	1.578E+27	1.471E+27	1.664E+27	123456	
E0	3.686E+27	3.491E+27	4.147E+27	3.915E+27	4.056E+27	4.894E+27	561234	

Fig. 3 Display of Tevatron parameters for a typical store.

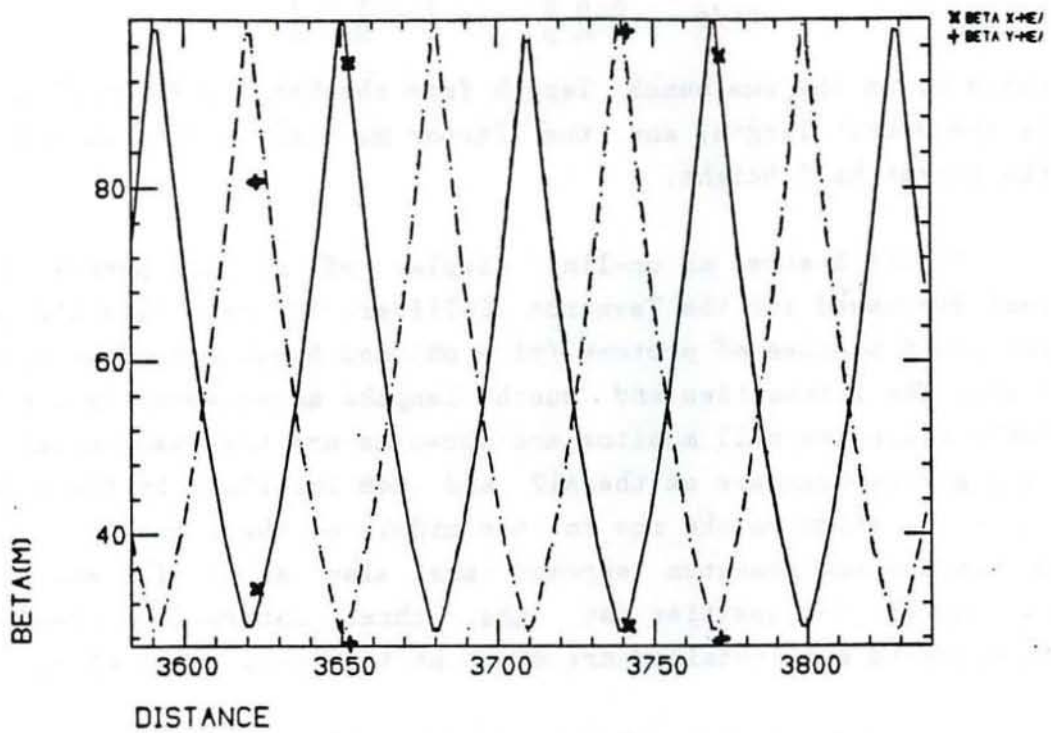


Fig. 4 Comparison of calculated and measured beta functions for the Tevatron injection or fixed target lattice.

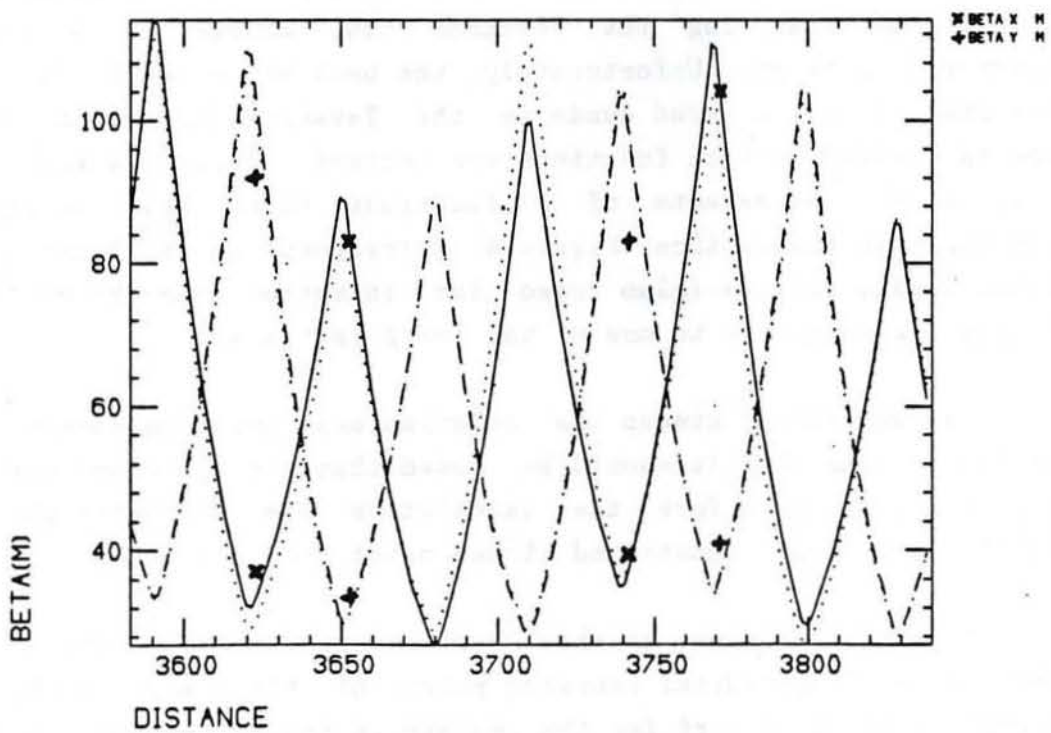


Fig. 5 The same as figure 4, but a low beta lattice.

The bunch momentum spread can be calculated to be

$$\Delta p/p = \frac{A h c}{8 R p} \sin \left[ \frac{\sigma_\lambda h}{R} \right],$$

where  $\sigma_\lambda$  is the rms bunch length from the Sampled Bunch Display,  $2\pi R/h$  is the bucket length, and the factor multiplying the sine function is the bucket half height.

Figure 3 shows an on-line display of all the parameters we have just discussed for the Tevatron Collider. The rows show the parameters for the 6 bunches of protons ( $p_1 - p_6$ ) and 6 bunches of antiprotons ( $a_1 - a_6$ ). The intensities and bunch lengths as measured from the Sampled Bunch resistive wall monitor are shown as are the measurements from the flying wire scanners at the A17 and C48 locations in the lattice. The units are shown on the row in the middle of the figure. The calculated emittances and momentum spreads are also shown for each bunch. The calculated luminosities at the three interaction regions where experiments are installed are shown at the lower right of the figure.

One of the most uncertain aspects of the calculations is in the knowledge of the lattice functions, not only at the IR, but also at the positions of the flying wires. If there were single quadrupoles at these important locations one could verify the beta function values directly by measuring the betatron tune change as a function of quadrupole strength. Unfortunately, the best we can do to is to use the few individually powered quads in the Tevatron lattice to verify that the calculated lattice functions are correct. Figures 4 and 5 show the results of measurements of  $\beta$  functions using this technique at 4 locations in the lattice. Figure 4 corresponds to the lattice used for fixed target physics (also used for injection into the collider) and figure 5 corresponds to one of the low  $\beta$  lattices.

The agreement between the calculations and measurements seems to be better than 10%. It should be noted that the agreement was worse by a factor of two before the calculation was done with the measured multipoles of all magnets and closed orbit errors included.

The beta functions at the low  $\beta$  IR were verified using a technique whereby the longitudinal crossing point of the  $p$  and  $p\bar{p}$  bunches was varied. That is, the rf for the protons is independent of the  $p\bar{p}$  rf

Relative Luminosity vs. Collision Point  
Model evaluated for various values of Beta\*

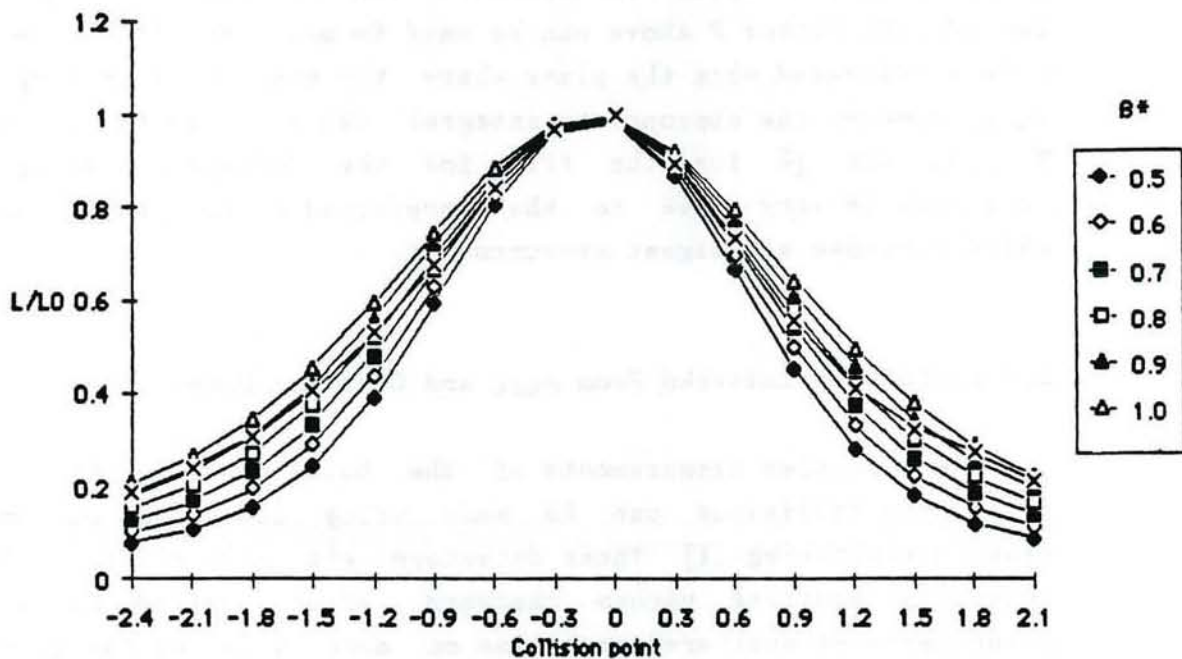


Fig. 6 Measured and calculated luminosity as a function of the longitudinal displacement of the crossing point of the p and pbar bunches. The measured points are indicated by the symbol x.

Chi-squared vs. Beta\* for various bunch lengths

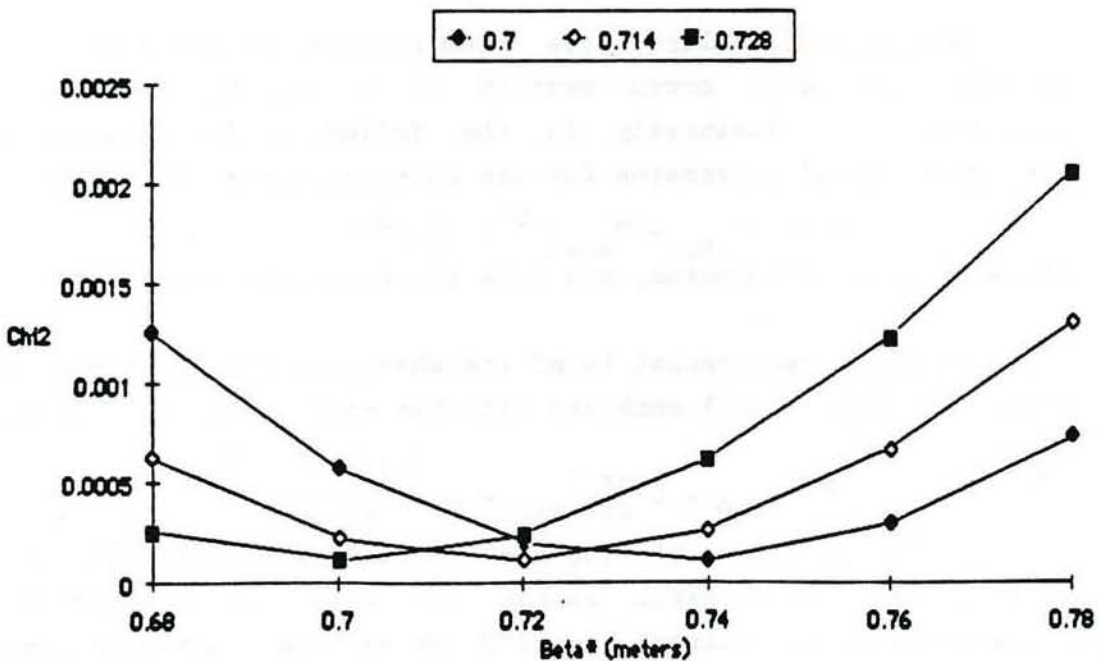


Fig. 7 Results of fitting the curves of Fig. 6 to determine the beta\* at the interaction point.

and the crossing point can be varied. Figure 6 shows the measured interaction rate as a function of the position of the central collision point as well as the results of calculations for different assumed  $\beta^*$ . A simple model which incorporates the equation for the luminosity degradation factor  $F$  above can be used to determine  $\beta^*$ . The equation is more complicated when the place where the beams meet is displaced from  $\beta_{\min}$ . However the appropriate integral can still be calculated. Figure 7 shows the  $\chi^2$  for the fits for the different assumptions. The agreement is very close to that predicted by the lattice calculation which included all magnet measurements.

## 2.2 Luminosity Inferred From $\sigma_{\text{tot}}$ and Counting Rates

Very precise measurements of the total cross section for proton-antiproton collisions can be made using detectors of small angle elastic scattering.[1] These detectors sit very close to the beam in specially modified vacuum chambers often called Roman Pots. A coincidence of scattered particles on each side of the IR with equal scattering angle,  $\theta$ , is used to identify an elastic event. Figure 8 is a schematic of such an experiment. Note that there are at least two sets of Roman Pots on each side of the IR, the farthest being well into the lattice to measure the smallest possible scattering angles.

There are actually three measurements which must be done to determine the total cross section in a way that is independent of knowledge of the luminosity. In the following discussion we shall use the conventional expression for the momentum transfer squared,  $t$ .

$$t \equiv (P_{\text{inc}} - P_{\text{scat}})^2 = 2 p^2 (1 - \cos \theta)$$

where  $P$  is the 4-momentum, and  $p$  is the beam momentum.

The first measurement is of the change in the scattering rate as  $t$  goes to 0. Equation 1) combined with the optical theorem yields:

$$\frac{dR}{dt} \Big|_{t=0} = L \frac{d\sigma}{dt} \Big|_{t=0} = L \frac{(1 + \rho^2) \sigma_{\text{tot}}^2}{16 \pi^2}$$

where  $\rho$  is the ratio of the real to imaginary scattering amplitudes. Clearly this measurement cannot be made at 0 degrees and an extrapolation is required. Figure 9 shows the scattering angle of the protons vs that of the pbars. The elastic scatters are easily seen. Figure 10 shows the measured differential cross section for experiment E710 at Fermilab.

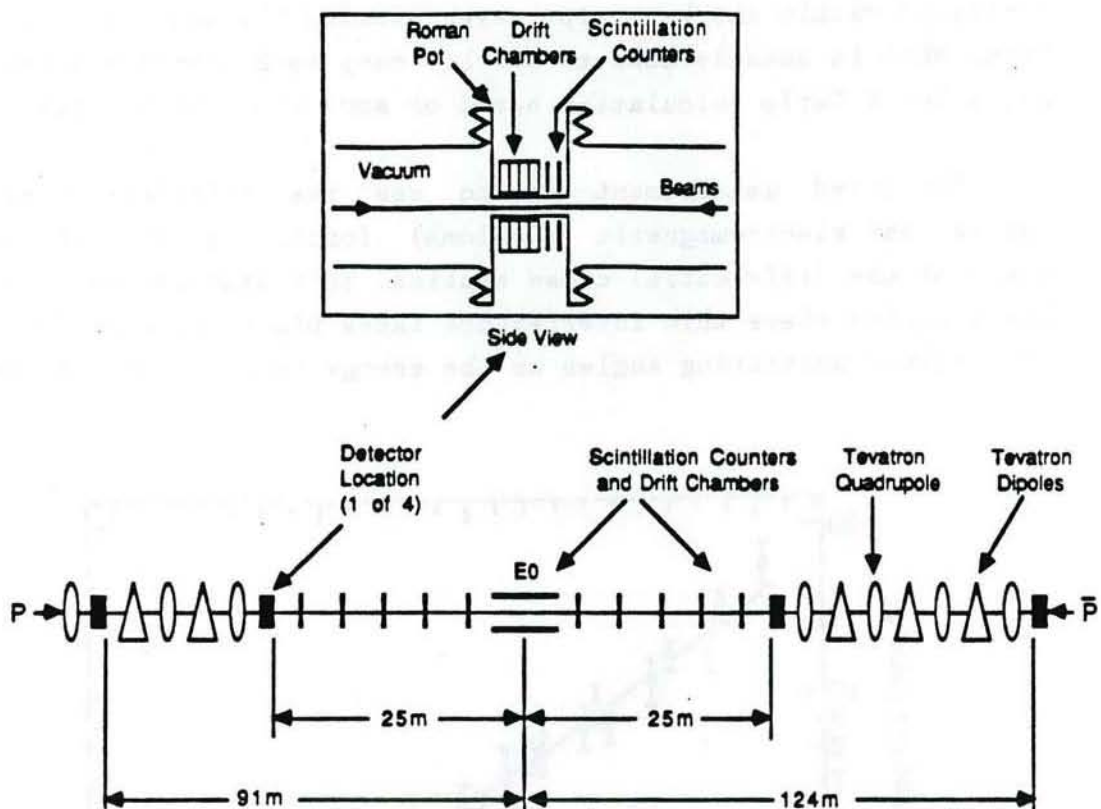


Fig. 8 Schematic diagram of the interaction region showing the locations of the Roman pots. The inset shows the location of the detectors in the pots.

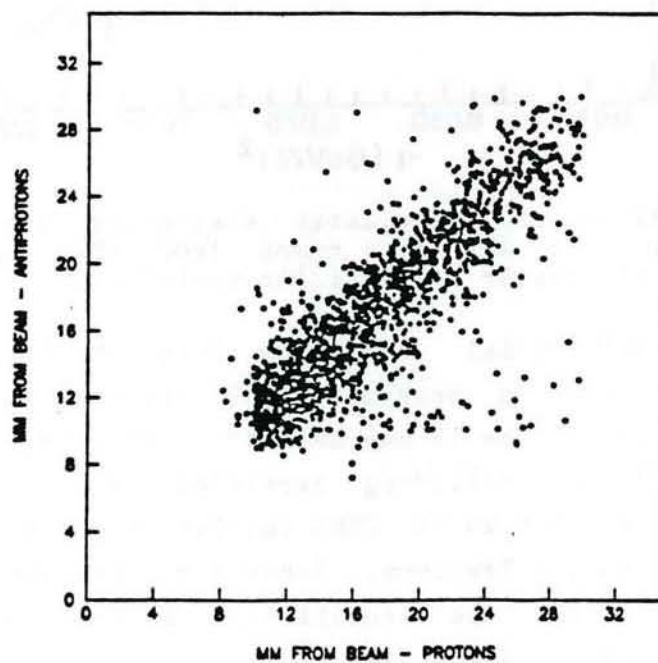


Fig. 9 Scatter plot of the displacement of the scattered protons on one side of the IR vs the displacement of the pbars on the other side.

The second measurement involves surrounding the IR with detectors to measure the total rate  $R$ , giving  $L\sigma_{\text{tot}}$ . Some events will be entirely contained within the beam pipe, even missing the detectors in the Roman Pots. What is usually done to see how many such events are missed is to use a Monte Carlo calculation based on some model of the interaction.

The third measurement is to see the interference between the nuclear and electromagnetic (Coulomb) forces in the details of the shape of the differential cross section. This measurement determines  $\rho$ . The  $t$  region where this interference takes place corresponds to smaller and smaller scattering angles as the energy is increased. At energies

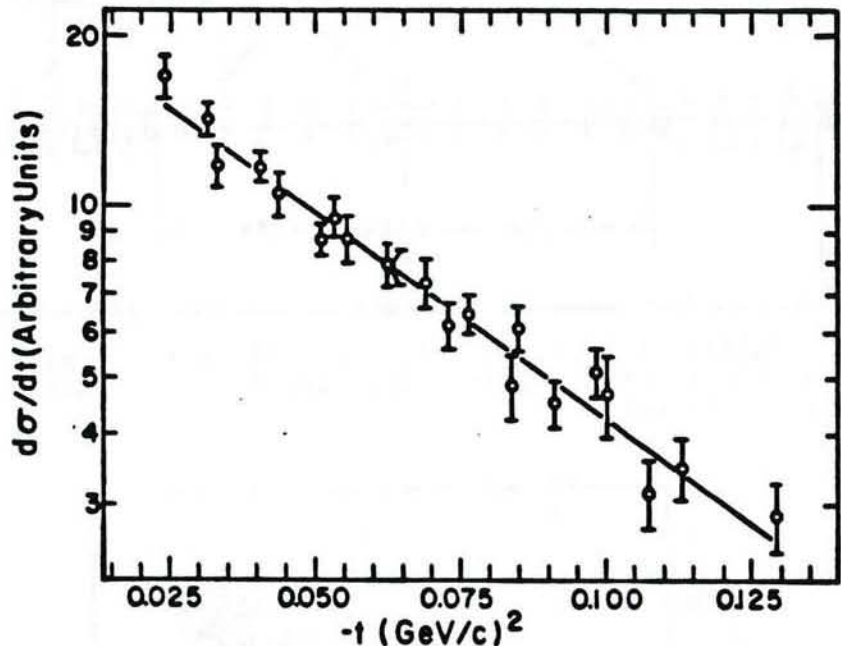


Fig. 10 Distribution of elastic scattering events as seen in the previous figure. The abscissa comes from the scattering angle, the ordinate from the number of particles within each angular interval.

approaching 1 TeV special conditions have to be used; the beams may have to be scraped to provide small transverse emittances and the lattice functions at the IR may have to be adjusted to provide parallel trajectories of the colliding particles. The value of  $\rho$  has been measured to be about 0.25 at CERN collider energies and is expected to be around 0.15 at the Tevatron. Since  $\rho$  enters into the expression for the luminosity as  $\rho^2$ , the sensitivity of the final answers to this parameter is somewhat diminished.

The three separate measurements can then be combined to give  $L$ ,  $\sigma_{pp}$ , and  $\rho$ . Unfortunately, the conditions for the most precise measurements are not those needed for the most popular operating conditions and more extrapolations are needed. For example, at Fermilab the best total cross section measurements are to be done at a different IR than the one with the major detectors. What should be possible is a precise measurement of the beam emittances as a consequence of the precise luminosity determination. The luminosity at the major detectors then depends primarily on a knowledge of the  $\beta$  functions in the low  $\beta$  regions of these major experiments.

### 3 ENERGY

#### 3.1 Spin Depolarization Resonance Method For $e^+e^-$ Machines

In an  $e^+e^-$  machine the energy calibration of the beams relates directly to the precision of the mass measurements of particles produced in collisions. Luckily there is a very sophisticated method for determining the absolute energy of  $e^+e^-$  machines. [2]

The beams in a collider can become polarized due to synchrotron radiation. A small spin-flip contribution is responsible for this polarizing effect which amounts to only one part in  $10^{11}$  of the total radiation. The polarization of the beam can be monitored by scattering a laser beam off the circulating beam and measuring the spin-dependent part of the Compton scattering by recording the angular distribution of the back-scattered  $\gamma$  rays.

The energy of the machine can be varied until a  $(g-2)$  resonance is excited which causes the beam to depolarize. Assuming the resonance can be uniquely identified, the spin tune  $\nu_s = \gamma(g-2)/2$  is determined. The beam energy is  $m_e\gamma$ . The largest source of error in this determination is in  $m_e$  which is known to 2.7 parts per million.

#### 3.2 Traditional Energy Determination by Magnetic Field Measurements

As stated before, the energy of a hadron collider is not as important as for an  $e^+e^-$  machine as far as high energy physics results are concerned. Nevertheless, one needs to know the value and how accurately the number is known. It may be instructive to examine the

details of the Tevatron energy determination.

In principle, the energy of the beam in the Tevatron could be measured by determining the speed of the particles. This takes knowing the path length and the transit time. Here, the path length is the circumference, as determined from the optical survey, and the transit time is the inverse of the revolution frequency which is determined from the rf frequency. While the circumference is probably known from optical surveys to better than a few centimeters (out of  $2\pi$  km) and the rf frequency can be measured to better than 1 Hz (out of 53 MHz), the problem is that the velocity of a 900 GeV particle is not a sensitive function of energy. This is a consequence of special relativity.

In units where  $c = 1$ ,  $E^2 = p^2 + m^2$ ,  $E = m\gamma$ , and  $p = m\beta\gamma$ ,

one can easily show that  $\frac{dE}{E} = \frac{p^2}{m^2} \frac{d\beta}{\beta}$ . Now suppose you could

measure the revolution period infinitely well but knew the circumference to 1 mm out of  $2\pi$  km, a rather remarkable precision even with the sophistication of modern survey techniques. Then for a momentum of 900 GeV/c ( $m_p = 0.938$  GeV/c $^2$ ), the fractional error on the energy determination would be over 10%.

A more sensitive method is to use the measured fields of the Tevatron magnets to determine the beam energy. That is, the total line integral corresponds to exactly  $2\pi$  radians of bend. It is fortunate that each of the Tevatron magnets was measured in some detail; many previous accelerators were built without such precise measurements.

An operator sets the energy of the Tevatron by entering the desired values in the T48 application program. This program downloads a table of values in Amperes to the power supply control microprocessor (TECAR) scaled by the factor 4.44 Amps/GeV. The factor was determined based on measurements of the very first Tevatron dipoles.[3] This factor is only  $1.5 \cdot 10^{-3}$  higher than our best estimate based on measurements of all the Tevatron dipoles.

The TECAR microprocessor system uses a precision transductor[4] to regulate the current to the table values. The specifications on the transductor are quite good, but the uncertainty introduced in the modifications needed to incorporate the device into the Tevatron turn out to be the limiting factor in the absolute energy determination of

the machine.

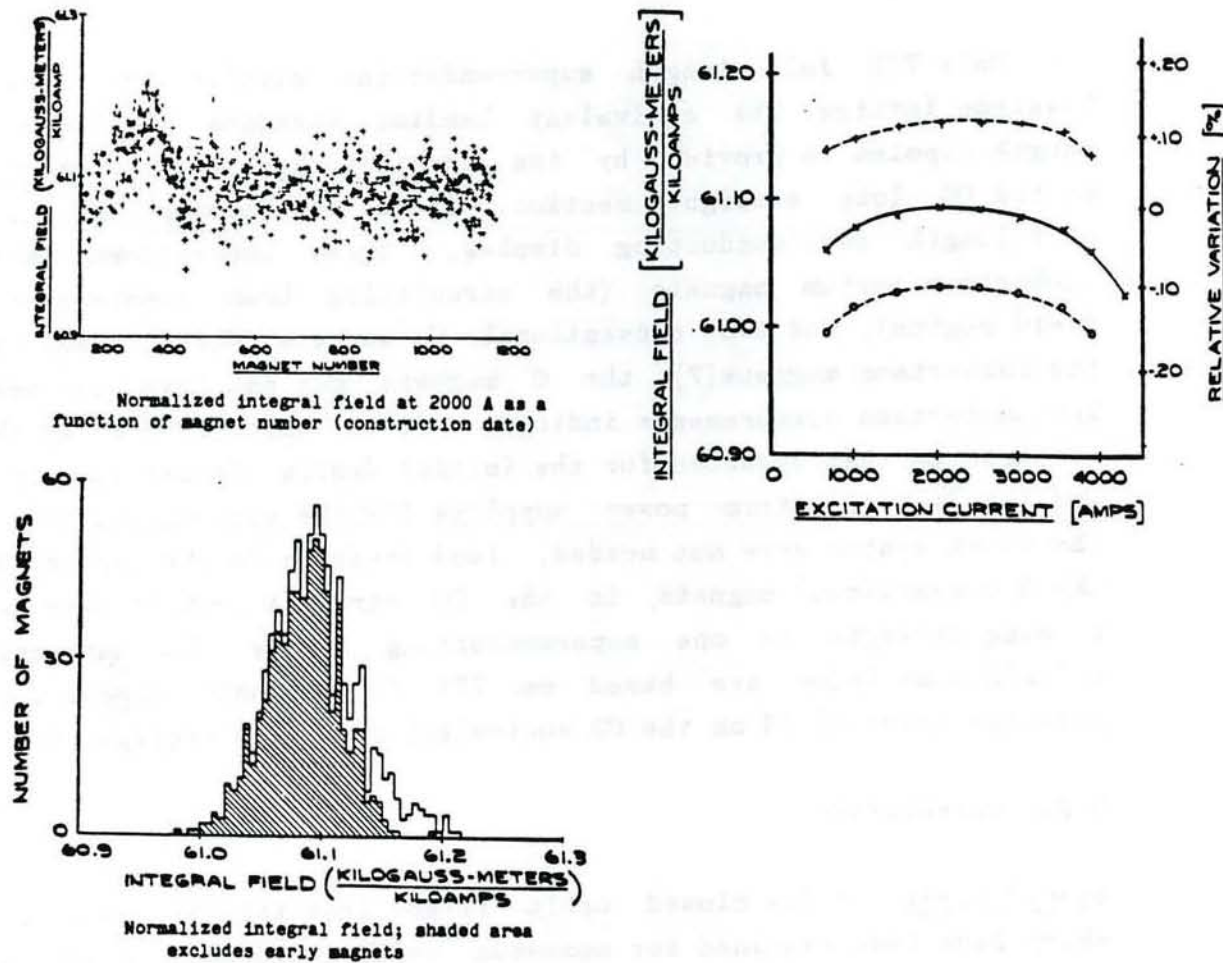


Fig. 11 Data from magnet measurements of the superconducting dipoles from reference [10]. The first figure shows the line integral of each magnet plotted as a function of magnet number. The second figure is a projection of the first figure, showing the distribution of excitation constants for the magnets. These data correspond to 2000 A excitation current. The third plot shows how the excitation field deviates from a linear function of current, presumably due to iron saturation and coil deformation.

### 3.2.1 Dipole Field Measurements

The results of integral field measurements of the Tevatron superconducting dipoles using a stretched wire loop have been published. [5] Figure 11 shows the results of the measurements. The average excitation function for the 870 measured dipoles is 61.09 kG-m/kA for a current of 2 kA. There is some dependence of the excitation function on the current; as the current approaches the 1 TeV level the

excitation function drops by 0.1%, presumably from yoke saturation and coil deformation. Besides these effects, a numerical error of -.03% which was discovered after publication has been included in the analysis. [6]

Only 772 full length superconducting dipoles are used in the Tevatron lattice. The equivalent bending strength of two more full length dipoles is provided by the special magnets of the abort system at the CO long straight section. These special magnets include two half-length superconducting dipoles, three conventional symmetric Lambertson septum magnets (the circulating beam passes through the field region), and two conventional C magnets. Whereas data exist on the Lambertson magnets[7], the C magnets may not have been measured. The Lambertson measurements indicate a field which is high by about 1% compared to that expected for the initial design. Geometric constraints and the fact that trim power supplies for the conventional magnets in the abort system were not needed, lend credence to the assumption that the 5 conventional magnets in the CO straight section have the same bending strength as one superconducting dipole. In any case, the calculations below are based on 774 full length dipoles, where a possible error of 1% on the CO equivalent magnet is negligible.

### 3.2.2 Corrections

closed orbit. A few closed orbit files from the '87 run still exist which have been examined for momentum errors. Figure 12 shows an orbit taken during a 900 GeV store at low beta. The average momentum displacement is -2.43E-4. Although the beam position monitoring system did not handle single rf bunches well, there is no reason to believe that the errors would produce or hide a systematic radial offset. Based on this assumption and the fact that an earlier 800 GeV store with 20 bunches shows the same offset, the energy reported below has been reduced by a factor of -2.43E-4.

dipole correction elements. The horizontal correction dipoles can provide additional bending strength to the Tevatron. Each correction dipole can provide 4.5974 kG-m at 50 Amps. Including 4 special horizontal dipoles at B0, the 112 correction dipoles in the ring had an average current of 6.6 Amps according to the T23 files for the 900 GeV low  $\beta$  stores. This leads to an energy correction of +.336 GeV.

These corrections apply only to the 900 GeV data. No orbits or

correction dipole ADC files remain for the 315 GeV data; the 315 GeV error has been increased accordingly.

### 3.2.3 Errors

Systematic errors in the magnet measurements include the geometry of the stretched wire probe ( $\pm 3E-4$ ), the shunt calibration ( $\pm 2E-4$ ), and the integrator time constant ( $\pm 3E-4$ ).

In addition there is a possible current error in the Tevatron due to uncertainties in the current regulator circuitry ( $\pm 1E-3$ ). As mentioned before, this error can be reduced by a factor of 3 or more by measuring the properties of the circuit. For this reason, this error is explicitly listed in the table below.

### 3.2.4 Results

Combining all corrections and errors except the current regulator error (shown in parentheses), the actual Tevatron energies for the '87 collider run were (in GeV, total);

<u>Nominal Energy</u>	<u>Calculated Energy</u>	<u>Systematic Error</u>
315	315.7	$\pm 0.1$ (0.3)
900	901.5	$\pm 0.2$ (0.9)

### 3.2.5 Discussion; Tevatron Radius

The beam energy has been determined from the measured fields of the bending magnets, where a bending angle of  $2\pi$  radians was used. The measured rf frequency ( $53104707 \pm 2$ ) Hz[8] determines the circumference or average radius of the closed orbit at 900 GeV.

$$R = \frac{h \beta c}{2 \pi f_{rf}} = 1000.0061 \text{ m}$$

This implies a very precise measurement of the average radius, where the error is determined by the error on the measurement of the rf frequency. An assumed frequency error of 2 Hz out of 53 MHz leads to a precision of better than  $40 \mu\text{m}$  on the determination of the radius. This can be compared to a measurement made during the earliest days of

Tevatron operation which essentially assumed that the transfer energy between the MR and Tevatron was well known.[9] This early measurement yielded a radius of 1000.006245 m  $\pm$  1 mm at 150 GeV.

An analysis of the magnetic field data was used to correct the Amp factor in the Tevatron low level rf system some years ago. The value coded into the K/I<sup>2</sup> box is 4.4287 compared to the original 4.44. The value at 900 GeV, based on the analysis in this paper for zero average horizontal correction dipole current, should be 4.4333.

For future measurements of the beam energy, it will probably be sufficient to make an accurate determination of the rf frequency and use the now well measured average radius of 1000.0061 m. The determination of the error of the Tevatron current regulation circuit should be improved, however, before the number is cast in stone.

### 3.3 Other Possibilities for Energy Determination.

The absolute calibration of an external beam line can be quite good. One especially interesting technique which uses elastic scattering of an extracted beam off of a gaseous helium target has been used up to 300 GeV at the SPS.[10] By simultaneously measuring the scattering angle,  $\theta$ , and the energy of the recoiling nucleus, TR, the determination of the four-momentum transfer is over-constrained:

$$\text{abs}(t) = (p\theta)^{**2} \quad \text{and} \quad \text{abs}(t) = 2 \text{ MR TR}.$$

The novel feature of this experiment, and the reason that the result is so precise, is the absolute calibration of the determination of the recoil energy. The helium target is also the ionization chamber used to measure the recoil energy. By using a radioactive  $\alpha$  source of energy  $E_\alpha$  and using events where  $TR = E_\alpha$ , one has an absolute calibration reference which does not rely on assumptions about the relation between ionization charge and recoil energy or about the linearity of the electronics.

The authors quote an error of 0.15% at 250 GeV with the expectation that the errors would be smaller at higher energy. While this method could not be used during colliding beam operation, requiring an extracted primary beam, it would allow the value of the machine energy to be calibrated absolutely without any assumptions

about the strengths of the magnets and the currents in them.

I thank the following people for valuable discussions concerning the subjects of this contribution: Chuck Ankenbrandt, Norm Gelfand, Gerry Jackson, Sateesh Mane, Roy Rubinstein, and Nicolay Terentyev. Thanks also to Chuck and Norm for providing figures.

#### 4 REFERENCES AND FOOTNOTES

- [1] N. Amos et al., Nucl. Instr. Meth. A252, 263(1986).  
N. A. Amos et al., FERMILAB-Pub-88/38-E.
- [2] A. S. Artamonov et al., Physics Lett. 118B, 225(1982).  
W. W. MacKay et al., Physical Review D29, 2483(1984).
- [3] "Beam Momentum vs Dipole Current in the Doubler", Sho Ohnuma, April 30, 1980, Memo.
- [4] Holec Zero Flux Current Transductor for Precise D.C. Measurement, type 5000 SH. This transductor has original factory specifications of 100 ppm absolute accuracy with an expected maximum error of 10 ppm change per month thereafter. In fact, as used in the Tevatron, the circuit has been altered such that the absolute calibration error is degraded to 0.1% (Dan Wolff, private communication). This error can be reduced by making the appropriate measurements.
- [5] R. Hanft, B.C. Brown, W.E. Cooper, D.A. Gross, L. Michelotti, E.E. Schmidt, F. Turkot, IEEE Vol. NS-30, No. 4, p 3381 (1983).
- [6] R. Hanft, private communication.
- [7] M. Harrison and F. N. Rad, "Symmetric and Non-symmetric Lambertson Magnets", FN-398, (Feb. 1984), and submitted to Nucl. Instrum. Methods. Figure 7 of this paper shows an excitation function which is a factor of 100 too large. With this correction, the values are thought to be correct (M. Harrison, private communication).
- [8] Keith Meisner, private communication.
- [9] Cordon Kerns, Quentin Kerns, and Harold Miller, IEEE NS-32, No. 5, p 1930 (1985).
- [10] J. P. Burq, et. al., NIM 177, (1980) 353-359.
- [11] For  $\eta_x$  non-zero, but neglecting  $\eta'x$ ,

$$L = \frac{f_{rev}}{4 \pi \sqrt{\beta_y}} \sum_{i=1}^n \frac{N_i \bar{N}_j F(\sigma_{\lambda i}, \sigma_{\lambda j}, \beta_x^*, \beta_y^*)}{\sqrt{\frac{1}{4} \left\{ \beta_x (\epsilon_{xi} + \bar{\epsilon}_{xj}) + \eta_x^2 \left[ \left[ \frac{\Delta p}{p_i} \right]^2 + \left[ \frac{\bar{\Delta p}}{p_j} \right]^2 \right] \right\} (\epsilon_{yi} + \bar{\epsilon}_{yj})}}$$

